IEEE Access
Multidisciplinary | Rapid Review | Open Access Journal

Received July 30, 2018, accepted September 2, 2018, date of publication September 10, 2018, date of current version October 8, 2018.

Digital Object Identifier 10.1109/ACCESS.2018.2869304

Spectral Efficiency Increase for Passive Backscatter Communication Based on Discrete Pulse Shaping

MANUEL FERDIK, (Student Member, IEEE), GEORG SAXL, DJORDJE GUNJIC, AND THOMAS USSMUELLER, (Senior Member, IEEE)

Microelectronics and Implantable Systems Group, Department of Mechatronics, University of Innsbruck, 6020 Innsbruck, Austria

Corresponding author: Manuel Ferdik (manuel.ferdik@uibk.ac.at)

This work was supported in part by the Austrian Research Promotion Agency (FFG) within the project "BaKoSens 4.0" under Grant 8633205 and in part by the University of Innsbruck.

ABSTRACT The Internet of Things comprises the network of billions of devices. The need for wireless systems is leading to bandwidth becoming an extremely limited resource. For this reason, the spectral efficiency of radio systems is playing an increasingly important role. While active radios already use pulse shaping techniques to improve the efficiency, passive systems still make a little use of them. The reason for this is that the energy available for shaping is very low and would, therefore, massively influence the range. This paper presents a concept that enables pulse shaping especially for passive "ultra-high-frequency radio frequency identification" transponders without significantly reducing the range at the same time. For this purpose, all approaches were designed to meet the requirements for chip integration. A 41-stage discrete Gaussian pulse was used which can be generated by a field-effect transistor. The transistor is controlled by a simple voltage divider which is operated by the digital part of the transponder. The total power consumption of the concept with simultaneously acceptable space requirement is estimated with 200 nW. The results of both the simulation and the measurements show that even a small number of steps improve the spectral efficiency. In adjacent channels, less energy is radiated compared with a rectangular pulse. According to the measurements, the adjacent channel power ratio in the directly adjacent channel for the discrete Gaussian is 7.5 dBc lower than for the rectangular shape. This effect is more pronounced with an increasing distance and is already 32 dBc for the fourth adjacent channel.

INDEX TERMS
Pulse shaping methods, RF signals, spectral analysis, UHF communication, radiofrequency identification, integrated circuit.

I. INTRODUCTION

The 'Internet of Things' - or short IoT - will have a massive impact on our future. This vision is shared by almost all experts. When trying to describe IoT, however, the minds diverge. There are many different approaches, most of which are strongly influenced by one's own research area. But still, all attempts to explain are united by the fact that it is based on a network of billions of devices. "50 billion devices in 2020" - this prediction was made by several experts in 2010 [1], [2]. In the meantime, this number has been revised and new estimates assume 30 billion by 2020 [3]. Nevertheless, the number of devices will be massive and the demands on the infrastructure accordingly high.

At first glance, a wired solution might seem attractive, but would come with serious drawbacks. Low flexibility and high cost for cabling will lead to low acceptance of wired systems in future scenarios. On the other hand, wireless communication convinces in exactly these areas. Flexibility, no cables and easy expansion lead to the great desire for wireless connection in the Internet of Things.

This variant has one major disadvantage though, namely the energy supply. Precisely, such a system implies that there is no cable available to connect the device to a power supply. In order to provide the energy for operation two possible solutions exist:

1) Battery: Each device has a battery on board which ensures the power supply.
2) Batteryless (passive): The devices generate their own power through energy harvesting.

The latter variant is preferable both from an ecological and economic point of view. For this reason, passive wireless networks (PWN) are the ideal answer to the changed requirements within the Internet of Things.

A promising technique to implement a PWN is Ultra High Frequency Radio Frequency Identification (UHF RFID). In recent years, this field of research has developed rapidly and now offers passive nodes with new functionalities such as sensors [4], [5] and actuators [6]. With ranges of around 10 meters passive UHF RFID meets all requirements to be a key technology and is therefore particularly interesting for IoT. Another challenge within the wireless IoT scenario is the shortage in the available radio spectrum. A large number of participants share a very limited frequency band. In order to avoid interference among devices and still ensure a simultaneous communication between several participants, spectral efficiency is inevitable.

The spectral efficiency of a signal depends on the in-band and out-of-band radiation. A rectangular pulse, which is a widespread shape in digital communication, leads to high side lobes in the frequency response and thus a large part of the transmitted power is out-of-band. Therefore, a rectangular shape is not desirable in terms of spectral efficiency. On the other hand, a signal with good spectral properties focuses the transmitted power within the transmission bandwidth. One way to increase spectral efficiency is pulse shaping. As the name suggests, this technique modifies the shape of the pulse to suppress out-of-band radiation and lower the power transmitted in the adjacent band [7].

Pulse shaping is already widespread in active radio systems to optimize the spectral efficiency [8], [9]. Although this technology already exists, it has not yet found its way into backscatter communication - such as UHF RFID. The reason is that with active radio systems the power supply is not a limiting factor and thus the hardware can be more complex. Therefore, filters can optimize the pulse shape as desired. In contrast, backscatter radios - like a passive UHF RFID transponder - only have simple circuitries. The analog front-end usually consists of few electronic components. For this reason, common concepts cannot be adopted without further ado.

In [10] and [11] an approach has been shown to take over pulse shaping in backscatter radios. Simple components like a p-i-n diode and a field effect transistor (FET) were used to generate a continuous, spectral efficient pulse shape. However, the disadvantage of the concept is that it is not suitable for passive UHF RFID. The continuous pulse shape can be generated in the demo setup, but this cannot be transferred to an integrated circuit without massively reducing the range of the system and thus limiting the area of application. The reason is that for a (quasi-) continuous shape a tag with an microcontroller unit [12] or a high-resolution and high-speed digital-to-analog converter is required. In passive UHF RFID $\sim$40 μW are available for the entire tag at a distance of 10 m [6]. So both options would require too much energy to ensure the desired reading range and therefore limit the use-cases.

In [13] a concept of a backscatter modulator with pulse shaping was presented, which is designed for WLAN at 5.8 GHz. A pulse shaping filter is used to optimize the hard edges followed by a switched resistor and capacitor bank. The problem again is energy consumption. The backscatter modulator chip requires 1.61 mW of power, which is orders of magnitude above the available energy in passive UHF RFID.

Since passive UHF RFID is an ideal candidate for communication in the Internet of Things, and spectral efficiency plays an enormous role, investigations in this area are highly interesting. In this paper a concept is proposed, which enables pulse shaping for passive UHF RFID with special regard to integrated circuit (IC) design. Due to the fact that pulse shaping is already in use within active radios, there are various investigations on the efficiency of different shapes [14]. Rectangle, Sinc, Raised Cosine and Gauss are very often compared in literature. Therefore, the aim is to investigate how a form can actually be integrated on a passive UHF RFID tag and at the same time have only minimal effects on its range due to the additional power requirements. The idea is to convert the continuous pulse into a sufficiently discrete pulse. The discrete stages can then be generated by specific switching of backscatter transistors. In the following, the Gauss pulse is examined in more detail. However, the concept itself can be applied to different types of pulse shapes.

II. PULSE SHAPE

A. CONTINUOUS PULSE

The shape of a typical rectangular pulse within UHF RFID is standardized in "EPCglobal Gen2 V2" [15] which determines timing, data rate and frequency. A typical data rate of 200 kbit/s leads to a pulse duration of $t_p = 5\,\mu$s. Therefore, this is the duration used in the following for the rectangular pulse:

$$y_{rec}(t) = \begin{cases} 1 & |t| \leq \frac{t_p}{2} \\ 0 & |t| > \frac{t_p}{2}. \end{cases} \tag{1}$$

It also determines the high time (power > 0.5) of the Gaussian shape:

$$y_{gauss}(t) = e^{\left(-\frac{1}{2}\left(\frac{t}{\sigma}\right)^2\right)} \; \sigma = \frac{t_p}{2.35}. \tag{2}$$

Figure 1 shows both signals in the time domain.

One way to characterize the spectral efficiency of a signal is the power spectral density (PSD) which indicates the power of a signal in an infinitesimal frequency band related to the frequency. Figure 2 illustrates that with increasing distance to the carrier frequency, the PSD of the Gaussian shape initially drops strongly before the curve flattens out. This effect is less significant with the rectangular pulse.

In order to quantize the effect not only for a specific frequency but for each channel in the band, an additional parameter is required. The adjacent channel power ratio (ACPR)

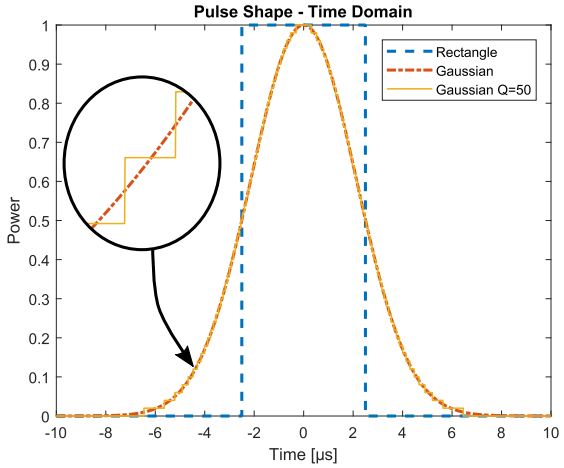

FIGURE 1. Used pulse shapes in the time domain. The blue line indicates the most common and widespread rectangular pulse. The red signal shows the spectral efficient continuous Gaussian pulse with the same high time (power > 0.5) as the rectangular. The quantized Gaussian signal (yellow) was generated with 50 steps.

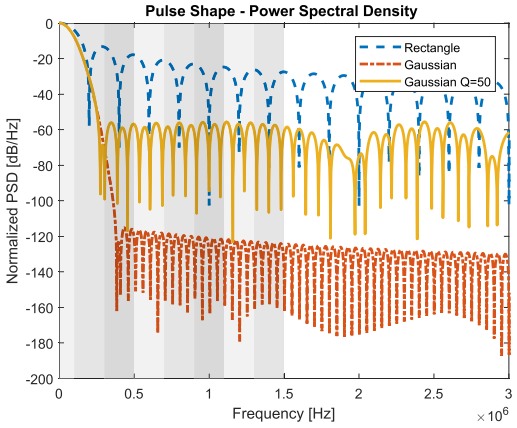

FIGURE 2. The spectral power density of the rectangular, Gaussian and the quantized Gaussian Pulse shape with 50 steps. The gray stripes in the background mark the available channels in the European UHF RFID frequency band from 865 MHz to 868 MHz (15 channels á 200 kHz).

indicates the ratio between the power P_{adj} in an adjacent channel and the power P_{main} in the main channel (#1):

$$ACPR_{dBc} = 10 \cdot \log_{10}\left(\frac{P_{adj}}{P_{main}}\right). \tag{3}$$

An ACPR of 0 dBc for an adjacent channel means that the same amount of energy is emitted in this channel as in reference channel 1. In contrast, an ACPR of −60 dBc means that 10^{-6} times less is radiated in the adjacent channel. In our case the parameter shows, that the effects of the pulse shaping is especially significant with more distant channels (Fig. 3). The ACPR difference in channel 2 is 3.8 dBc while in channel 4 it increases to 48.4 dBc. However, in all adjacent channels the Gaussian signal radiates less energy and is therefore the more efficient pulse shape.

B. DISCRETE PULSE

Continuous pulse forms cannot be realized in passive systems without influencing functionality like reading range.

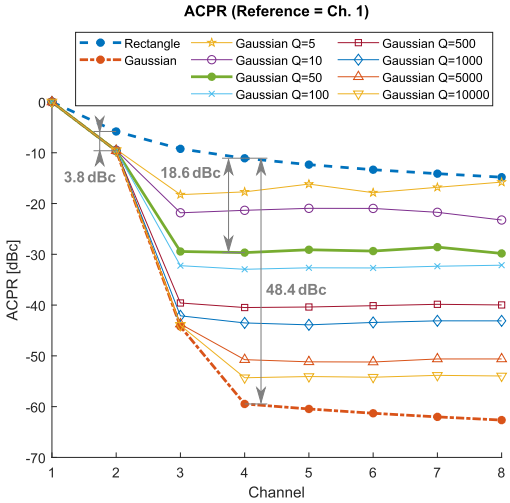

FIGURE 3. ACPR of the continuous rectangular and Gaussian pulse as well as discrete Gaussian shapes with various quantization steps between. More steps lead to an approximation towards the continuous Gauss and less steps towards the rectangular pulse. In all adjacent channels, the Gaussian shapes radiate less energy than the rectangular. The effect is more pronounced with more distant channels.

For this reason, a compromise between spectral and energy efficiency must be reached. The solution is to convert the continuous pulse into a discrete pulse y^*:

$$y^*_{gauss}(t) = \mathrm{sgn}(y_{gauss}(t)) \cdot \Delta \cdot \left\lfloor \frac{|y_{gauss}(t)|}{\Delta} + \frac{1}{2} \right\rfloor. \tag{4}$$

The trade-off between spectral and energy efficiency can be flexibly adjusted via the number of quantization steps and the corresponding step size Δ. A high number of steps leads to an approximation towards the continuous form and reaches it when $\Delta \to 0$. In contrast, a Gaussian pulse with one step equals a rectangular pulse.

This fact can also be seen in the ACPR. Figure 3 shows the curves for multiple quantization steps in the range between 5 and 10.000. Already 50 steps influence the spectral efficiency significantly and lead to an ACPR of −30 dBc from channel 3 onward. Thus, 50 steps are set as desirable target values in the following. The corresponding signal in the time domain and the PSD plot are shown in Figure 1 and 2. The exact number can only be determined on the basis of measurements and the actual properties of the components used.

III. PROPOSED SYSTEM

UHF RFID is based on the so-called backscatter technique. Data is not actively sent back from the transponder to the reader. Instead, the reflection coefficient Γ is systematically varied to switch between the two states matched and un-matched. When matched (Γ_m), the transponder does not reflect the incident wave and all energy is absorbed. In contrast, the electromagnetic wave of the reader is reflected in the un-matched state (Γ_{um}) and only little energy is absorbed. This principle allows the transponder to send back data to the reader.

However, more than two states are required to realize a quantized Gauss pulse. Therefore, a new transmission

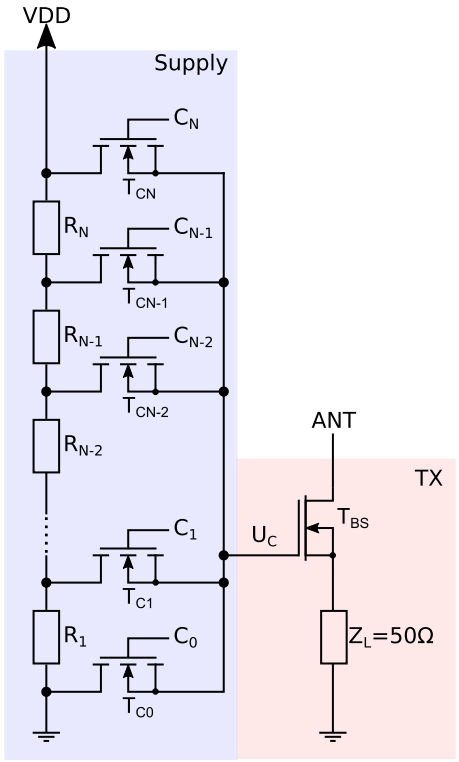

FIGURE 4. Proposed Concept of the pulse shaped backscatter system. The load impedance Z_L simulates the perfectly matched transponder at the antenna (ANT). The backscatter transistor T_{BS} which is used to adjust the grade of mismatch is controlled by the voltage U_C. The supply part is a simple voltage divider which generates the needed U_C. The transistors T_{CX} are used to connect through the desired value.

circuitry is required. The proposed concept is shown in Figure 4. The TX part consists of a load impedance Z_L which simulates the perfectly matched transponder. The depletion mode metal-oxide-semiconductor field-effect transistors (MOSFET) T_{BS} is used to generate a targeted mismatch depending on the control voltage U_C. In the extreme positions of T_{BS} the transistor either connects through or blocks. The quantization steps and therefore the grade of reflection can be adjusted with U_C.

To generate the control voltage a simple voltage divider is used. On the IC the resistors R_1 to R_N will be serial and parallel connection of unit resistors to achieve the desired values as accurately as possible. The enhancement mode MOSFETs T_{C0} to T_{CN} are used as switches to adjust U_C to the desired value. The control signals C_X are provided by the digital part of the transponder.

IV. MEASUREMENT SETUPS

A. DEVICE UNDER TEST

The device under test (DUT) shown in Figure 5 is set up on a printed circuit board (PCB). As material a 'Panasonic R-1566 FR4 Laminate' [16] is utilized. The entire circuit is designed to be as small as possible in order to avoid undesired RF effects. The SMA connector serves as input for the 866 MHz continuous wave (CW) from the reader and simultaneously as output for the reflected wave. As backscatter

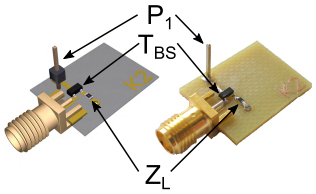

FIGURE 5. Prototype of proposed concept build on a PCB. On the left side the virtual model and on the right side the hardware prototype. The pin P_1 serves as interface for the control voltage U_C. The backscatter transistor T_{BS} is connected to a SMA jack. The load impedance $Z_L = 50\ \Omega$.

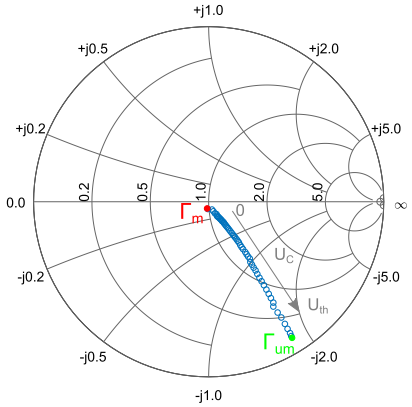

FIGURE 6. S_{11} Parameter for 58 U_C steps ranging from 0 V to U_{th} plotted in a Smith chart. When $U_C = 0$ V the DUT is matched (red mark) and no reflection occurs. At $U_C = U_{th}$ the DUT is mismatched (green mark) and only little energy is absorbed.

transistor an 'NXP BF1107 n-channel single gate depletion type' [17] HF MOSFET is used. The control voltage U_C is provided through pin P_1.

B. FINAL PULSE SHAPE

After the DUT was manufactured and assembled, first characterization tests were performed. A connection to a 'R&S ZNB8' vector network analyzer (VNA) is established via the SMA port and 58 different control voltages U_C were applied via pin P_1. The S_{11} parameter was measured over the entire UHF RFID frequency band from 865–868 MHz with the VNA. The results for 866 MHz is shown in the Smith chart in Figure 6.

As required, the matched state (Γ_m) and the un-matched state (Γ_{um}) are as far apart as possible. With a control voltage of $U_c = 0$ V, S_{11} is in the center of the chart. Therefore no reflection takes place and all energy is absorbed. In contrast, at $U_c = U_{th}$, $S_{11} = 0.46 - i0.79$ and causes a reflection and thus only a small part of the energy is absorbed (because of the passive operation mode of the tag, zero absorption is not wanted).

These results are used to determine the control voltages and the corresponding timings and thus to generate the Gaussian pulse. Of the 58 reflection points recorded, only 41 were required. The control voltage and the associated pulse over time are shown in Figure 7.

C. SETUPS

For the measurement setups shown in Figure 8 the supply part from the concept was emulated by a 'Keysight 81150A pulse

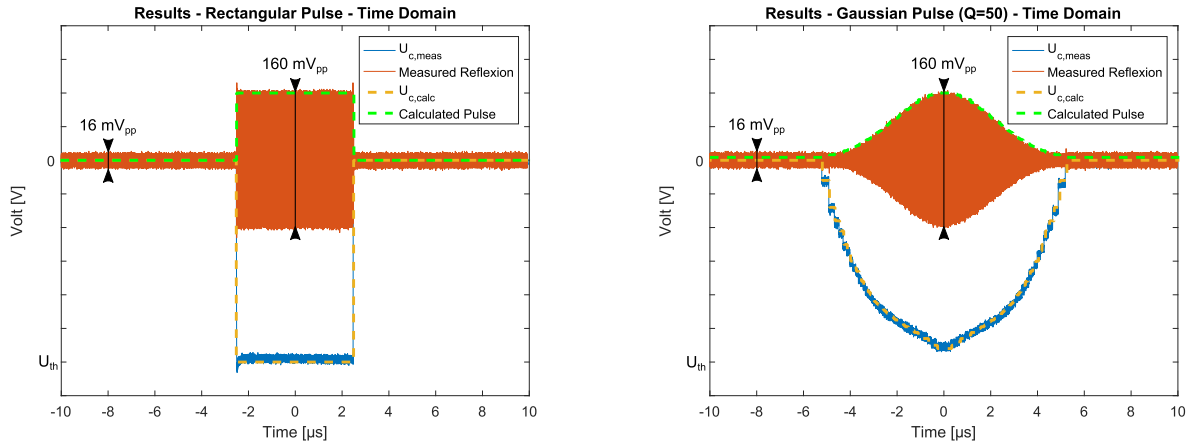

FIGURE 7. The calculated control voltage U_C (yellow) based on the results shown in Fig. 6 and the corresponding Pulse (green) are shown for the rectangular pulse (left) and the Gaussian pulse (right). The measured U_C (blue) and reflexion(red) are also plotted and show good agreement.

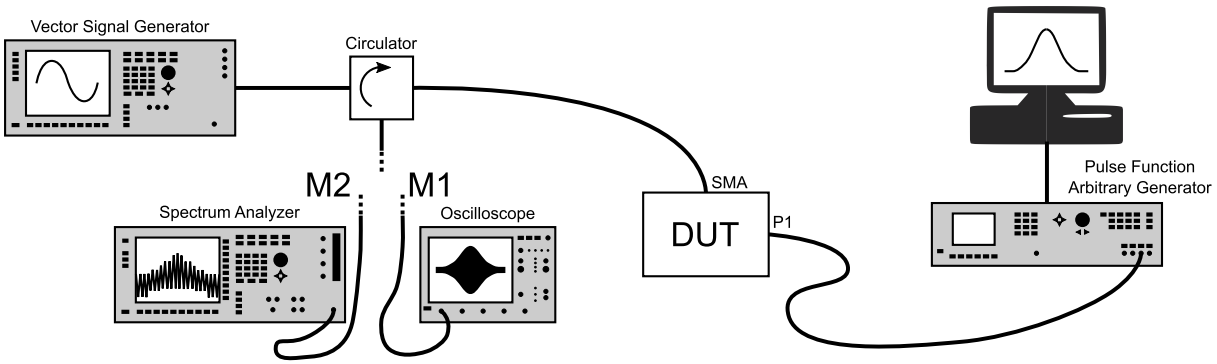

FIGURE 8. Schematic representation of the measurement setups. The control voltage U_C is provided over the pin P_1 by a computer controlled pulse function arbitrary generator. A vector signal generator simulates the 866 MHz CW signal of a reader. To simultaneously supply and measure the DUT, a circulator is needed. Two different measurements were performed. M1: spectral analysis, M2: time domain.

function arbitrary generator (PFAG)'. Therefore, the before calculated time course of U_C for a rectangular pulse and for a 41 steps quantized Gaussian pulse was programmed on the PFAG and transmitted to P_1 of the DUT. The 866 MHz and 0.2 V_{pp} CW signal - which under real conditions will be emitted by a reader and received by an antenna - is generated by a 'R&S SMU 200A vector signal generator (VSG)'.

In order to simultaneously supply the DUT and measure the reflexion, a coaxial circulator is connected between VSG and DUT. Two different measurements are performed:

- **M1** - Time Domain: In this measurement setup, the third port of the circulator is connected to a 'LeCroy WaveSurfer 104MXs-B 1GHz Oscilloscope'. The Oscilloscope monitors the reflection in the time domain.
- **M2** - Frequency Domain: For the frequency domain of the reflexion, the circulator is connected to a 'R&S 3.6 GHz FSU Spectrum Analyzer'. This allows statements to be made about the spectral efficiency.

V. RESULTS

A. TIME DOMAIN

With the setup M1, the reflection over time is examined more closely. The results are shown in Figure 7. The reflected pulse is modulated on the 866 MHz carrier wave and the envelope perfectly matches the calculated reflection. This is based on the control voltage Uc, whereby measurement and calculation are also in good agreement. From the generated 200 mV_{pp} CW signal in the unmatched state about 160 mV_{pp} and in the matched state 16 mV_{pp} are measured at the oscilloscope.

The observation in the time domain ensures that the pulse generation works as expected. However, it does not directly allow any statements to be made about spectral efficiency. Therefore, the frequency domain is examined in more detail below.

B. FREQUENCY DOMAIN

For the analysis of the spectral efficiency the measurement setup M2 shown in Figure 8 is used. The spectrum analyzer records the one-sided spectrum around the carrier frequency and delivers the results in Figure 9. The green and orange lines mark the calculated PSD for the rectangular and Gaussian pulse. The measured results are shown in blue and red.

The results of the rectangular pulse match perfectly with the simulation. Graphically, the curves are different, since a pulse sequence with 50 kHz was used for the measurement, while only one pulse was considered for the calculation. Thus, the calculated spectrum forms a kind of envelope of the measurement results.

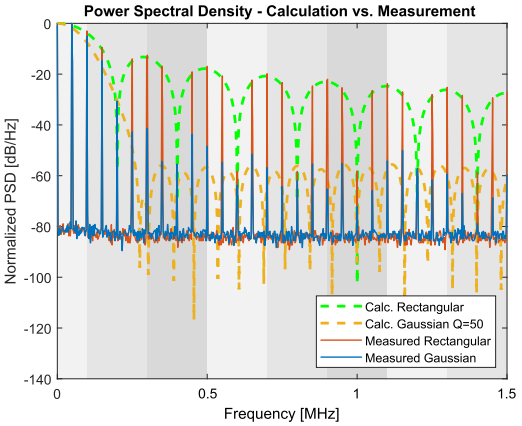

FIGURE 9. Comparison of the calculated to the measured PSD. The calculated results for the rectangle and the Gauss are shown in green and yellow. Red and blue represent the measurement. The peaks in the measurement result from the use of a pulse sequence with 50 kHz, while only one pulse was examined in the calculation.

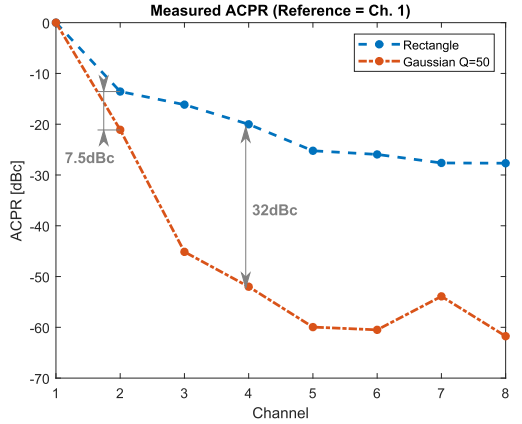

FIGURE 10. ACPR of the two measured pulse forms for 8 adjacent channels. The results for the rectangle pulse flatten very quickly in contrast to the Gaussian pulse. This results in an improvement of 32dBc already with channel 4.

The situation is similar with the Gauss pulse. Since 50 steps were assumed for the simulation and only 41 were used for the actual realization, there is a certain deviation of the results. Nevertheless, it can be seen that less energy is emitted in the adjacent channels. The ACPR is plotted in Figure 10 to quantize this positive effect. Already in the directly adjacent channel an improvement of 7.5 dBc when using a Gaussian shape quantized with 41 steps can be seen. The effects are more pronounced with increasing distance. In the fourth channel there is an improvement of 32 dBc.

C. ESTIMATION OF ENERGY CONSUMPTION

As presented in the measurement setups, the supply part of Figure 8 was replaced by a PFAG. In chip integration, this would be implemented as shown in the form of a voltage divide. Since this part contributes significantly to the energy consumption of the entire pulse shaping circuit, it must also be taken into account in the estimation. Transistor switching currents and leakage currents can be neglected.

In general, a high resistance is to be preferred, since this would cause a lower current and thus less loss. However, large resistors require a lot chip area. A certain compromise is therefore needed here. If a target value of 200 nA at 1 V V_{DD} is assumed, this would lead to a total resistance of 50 MΩ. On a 55 nm process of Globalfoundries a poly-resistor with this value would lead to an area requirement of 100 μm × 62 μm. Since the circuit consists not only of one single resistor but a voltage divider consisting of standard resistors connected to get certain values, the circuit is expected to require slightly more area.

This means that the total size is not larger than a single bond pad on the chip. With an energy consumption of 200 nW, the circuit is very well suited for use in passive UHF RFID transponder.

VI. CONCLUSION

This paper shows a way to use pulse shaping techniques - which are already used for active radios - in passive UHF RFID transponders without significant impact on its range. Common approaches are based on the realization of a continuous pulse which involves the use of extensive hardware and therefore increases power consumption drastically. The presented approach of a quantized pulse offers the possibility to make a compromise between spectral and energy efficiency by using only 200 nW. The required control voltage can be realized on the chip by a simple voltage divider. Even a few stages reduce the energy radiated in all adjacent bands significantly. The 41 steps quantized Gaussian pulse realized in this paper improves the ACPR compared to a rectangular pulse in the directly adjacent channel by 7.5 dBc and in channel 4 by 32 dBc.

Future work will deal with the use of multiple backscatter transistors. By using more than one transistor, it is possible to generate more stages and therefore to achieve a higher resolved pulse. Both series and parallel connections can be used. In the proposed concept (see Figure 4), the transistor T_{BS} is connected to the load impedance Z_L in series. When T_{BS} connects through, the antenna is matched to the transponder. When T_{BS} blocks, the system is un-matched. The same can be performed by connecting a transistor parallel to the load impedance. This time the transponder is matched, when the transistor blocks and un-matched when it connects through.

Furthermore, the presented concept can be utilized to create a flexible digital adjustment of the reflection stages. This means the digital part of the transponder can switch between different numbers of stages depending on the energy available. If very little energy is provided, only one stage and thus a common rectangular shape comes to use. In case enough energy is available, the digital part can utilize the maximum number of stages (depending on the voltage divider) to generate a Gaussian pulse. In between the digital part can flexible adjust the numbers and therefore affect the energy consumption.

Since the concept presented can provide any type of pulse shape, it is intended to serve as a basis for further investigations in this field. Due to the many advantages of passive

UHF RFID in combination with the presented pulse shaping technology, there are good chances it will prevail over active radios as a key technology in the Internet of Things.

REFERENCES

[1] D. Evans, "The Internet of Things: How the next evolution of the Internet is changing everything," Cisco Internet Bus. Solutions Group, San Jose, CA, USA, White Paper, 2011. [Online]. Available: https://www.cisco.com/c/dam/en_us/about/ac79/docs/innov/IoT_IBSG_0411FINAL.pdf

[2] H. Vestburg, "CEO to shareholders: 50 billion connections 2020," Ericsson, Stockholm, Sweden, 2010. [Online]. Available: http://mb.cision.com/Main/15448/2246220/662223.pdf

[3] *Ericsson Mobility Report: On the Pulse of the Networked Society*, Ericsson, Stockholm, Sweden, 2015.

[4] G. Chakaravarthi, K. P. Logakannan, J. Philip, J. Rengaswamy, V. Ramachandran, and K. Arunachalam, "Reusable passive wireless RFID sensor for strain measurement on metals," *IEEE Sensors J.*, vol. 18, no. 12, pp. 5143–5150, Jun. 2018.

[5] Y. Hu, J. Li, M. Yang, and S. Shuang, "Temperature prediction and fault diagnosis of primary equipment based on UHF—RFID sensor," in *Proc. 32nd Youth Acad. Annu. Conf. Chin. Assoc. Automat. (YAC)*, May 2017, pp. 269–271.

[6] M. Ferdik, G. Saxl, and T. Ussmueller, "Battery-less UHF RFID controlled transistor switch for Internet of Things applications—A feasibility study," in *Proc. IEEE Top. Conf. Wireless Sensors Sensor Netw. (WiSNet)*, Jan. 2018, pp. 96–98.

[7] S. Kumar, *Wireless Communication-the Fundamental and Advanced Concepts* (River Publishers Series in Communications), vol. 41. Aalborg, Denmark: River, 2015.

[8] S. Singh, M. Sharique, and A. A. Moinuddin, "PAPR reduction in SC-FDMA using transmit pulse shaping," in *Proc. Int. Conf. Multimedia, Signal Process. Commun. Technol. (IMPACT)*, Nov. 2017, pp. 275–279.

[9] J. G. Proakis and M. Salehi, *Digital Communications*, 5th ed. Boston, MA, USA: McGraw-Hill, 2008.

[10] J. Kimionis and M. M. Tentzeris, "Pulse shaping: The missing piece of backscatter radio and RFID," *IEEE Trans. Microw. Theory Techn.*, vol. 64, no. 12, pp. 4774–4788, Dec. 2016.

[11] J. Kimionis and M. M. Tentzeris, "Pulse shaping for backscatter radio," in *Proc. IEEE MTT-S Int. Microw. Symp. (IMS)*, May 2016, pp. 1–4.

[12] A. P. Sample, D. J. Yeager, P. S. Powledge, and J. R. Smith, "Design of a passively-powered, programmable sensing platform for UHF RFID systems," in *Proc. IEEE Int. Conf. (RFID)*, Mar. 2007, pp. 149–156.

[13] A. Tang, Y. Kim, Y. Xu, and M.-C. F. Chang, "A 5.8 GHz 54 Mb/s backscatter modulator for WLAN with symbol pre-distortion and transmit pulse shaping," *IEEE Microw. Wireless Compon. Lett.*, vol. 26, no. 9, pp. 729–731, Sep. 2016.

[14] P. M. Shankar, *Fading and Shadowing in Wireless Systems*. Cham, Switzerland: Springer, 2017.

[15] GS1 EPCglobal, *EPC Radio-Frequency Identity Protocols Generation-2 UHF RFID, V2: Specification for RFID Air Interface*, Nov. 2013.

[16] Panasonic Ind. Devices, *R-1566 Laminate*, 2017.

[17] NXP. (23007). *Bf1107 Data Sheet*. [Online]. Available: www.nxp.com/docs/en/data-sheet/BF1107.pdf

MANUEL FERDIK (S'16) was born in Schwaz, Austria, in 1989. He received the B.Sc. and Dipl.Ing. degrees in mechatronics from the University of Innsbruck, Austria, and the M.Sc. degree in industrial engineering from the Management Center Innsbruck, Austria. He is currently pursuing the Ph.D. degree with the University of Innsbruck. Since 2014, he has been a University Assistant with the University of Innsbruck and is a part of the Microelectronics and Implantable Systems Group. His research interests include batteryless and wireless sensor as well as actuator networks with special focus on UHF RFID.

GEORG SAXL was born in Innsbruck, Austria, in 1990. He received the B.Sc. and Dipl.Ing. degrees in mechatronics from the University of Innsbruck, Innsbruck, in 2016, where he is currently pursuing the Ph.D. degree in microelectronics. Since 2016, he has been a Research Assistant with the Microelectronics and Implantable Systems Department, Institute of Mechatronics, University of Innsbruck. His research interests include ultra-low-power circuits, systems for RF identification, passive wireless sensor networks, and chip design.

DJORDJE GUNJIC was born in Innsbruck, Austria, in 1994. He graduated from the Higher Institute for Technical Education in Electronics, Innsbruck, in 2014, with a specialization in telecommunications. He is currently pursuing the degree in mechatronics with the University of Innsbruck, where he is also involved in his bachelor's thesis.

THOMAS USSMUELLER (S'07–A'09–M'12–SM'13) was born in Nuremberg, Germany, in 1981. He received the Dipl.Ing. and Dr.Ing. degrees in electrical engineering from the University of Erlangen-Nuremberg, Erlangen, Germany, in 2006 and 2011, respectively. In 2006, he joined the Institute for Electronics Engineering, Erlangen, as a Research Assistant. From 2007 to 2014, he was a Teaching Fellow and the Head of the Chip Design Group, Institute for Electronics Engineering. Since 2014, he has been a University Professor with the University of Innsbruck, Innsbruck, Austria, where he currently leads the Microelectronics and Implantable Systems Group. He has authored or co-authored one book, two book chapters, and over 70 technical publications. His research interests include circuits and systems for RF identification, analog-to-digital and digital-to-analog converter design, and analog signal conditioning circuits. He is also interested in RF circuit design for ultra-wideband and cellular applications.